Analytical Approach to Predict the Magnetic Field of Slotted Permanent Magnet Linear Machines in Open-Circuit mode

Original Scientific Paper

Naghi Rostami*
Faculty of Electrical and Computer Engineering,
University of Tabriz, Tabriz 51666, Iran
29 Bahman Blvd., Tabriz, Iran
n-rostami@tabrizu.ac.ir

Amjed Alwan Albordhi
Faculty of Electrical and Computer Engineering,
University of Tabriz, Tabriz 51666, Iran
29 Bahman Blvd., Tabriz, Iran
amjed.albordi@tabrizu.ac.ir

Mohammad Bagher Bannae Sharifian
Faculty of Electrical and Computer Engineering,
University of Tabriz, Tabriz 51666, Iran
29 Bahman Blvd., Tabriz, Iran
sharifian@tabrizu.ac.ir

*Corresponding author

Abstract *– This paper presents an effective method to calculate the magnetic field distribution of slotted Permanent Magnet Linear Synchronous Machines (PMLSM) with surface-mounted magnets at no-load condition. 2D analytical expressions are employed to make a prediction of magnetic field components. The method proposed in this article has significant advantages in terms of accuracy compared to related studies. More harmonics can be included with new modifications in the analytical calculations. As a result, a more accurate field prediction is obtained. In addition, slot effects are considered in the prediction of the magnetic field. Finite element method (FEM) is used to assess the accuracy of the method.*

Keywords: *PMLSM, analytical method, field calculation, FEM*

Received: October 22, 2024; Received in revised form: June 23, 2025; Accepted: June 26, 2025

1. INTRODUCTION

Due to having many features such as high power density, simple structure, direct drive capability, the application of PMLSMs is expanding in various fields such as high-speed trains, CNCs, robotic arms, printing and dispensing, pick and place, and engraving or cutting equipment [1, 2].

Commonly, two different numerical and analytical methods are used to design electric machines [3]. Although numerical methods, such as the Finite Element Method (FEM) [4], can calculate the critical quantities of the machine considering its actual geometry, they cannot be effective in combination with iteration-based optimization techniques due to their time-consuming nature. Analytical calculation, if feasible, can be used as a significant tool in simplifying the problem and reducing the computational volume.

In [5], an analytical method based on equivalent magnetization intensity has been presented taking the spatial harmonics into account. In [6], the Magnetic Flux Density (MFD) distribution is predicted by an image method and a surface magnetic charge model for an air-core linear motor. A segmented conformal mapping method has been presented in [7] to predict the MFD distribution of a PMLSM. Although this method is fast

compared to FEM and its calculations are sufficiently accurate, the computation time is slightly high due to the presence of iterative loops. Another approach based on an equivalent surface current method is introduced in [8] for the magnetic field analysis of a PMLSM with trapezoidal halbach arrays. The presented method is quite simple, but its accuracy could be increased. In [9], to reduce the total computation time of a U-shaped PMLSM, most of the FEM steps are replaced by a non-linear equivalent circuit. Rahideh et al. [10] have performed analytical magnetic field calculations considering different magnetization patterns of slot-less PMLSMs. However, the calculations are not applicable for slotted linear motors. A new analytical approach is presented in [11] to calculate the MFD distribution and force of PMLSMs. The calculations have been accomplished assuming that the mover of the PMLSM is like a circle with an infinite radius of curvature. For a double-sided coreless PMLSM, an analytical model combined with an optimization technique is presented in [12]. Similar to [11], this model cannot be used to predict the MFD distribution of PMLSMs comprising a slotted stator core.

Despite the aforementioned advantages of analytical modeling, there are no sufficient studies carried out on the topic. Most of the reported studies in this field have focused on field calculations of core-less or slot-less linear motors or have presented complex methods that involve heavy mathematical calculations and empirical coefficients. This paper intends to provide an accurate method for calculating the MFD of slotted PMLSMs at open-circuit condition, which can be used in calculating other fundamental quantities of the machine, such as induced back-EMF and produced cogging force.

Briefly, the main content of this article is as follows.

- Considered model has been divided into several subdomains: 1) mover core; 2) magnets; 3) air gap; 4) slots; 5) stator core.
- The equations governing considered regions are expressed.
- The exact 2-D analytical approach is used to solve the Partial Differential Equations (PDEs).
- Boundary conditions are applied to obtain unknown integration constants.

It is noted that although some recent works employ analytical models for machine design problems [7, 8], the proposed framework in this paper has significant advantages in terms of the accuracy of the model due to adding slot effects in magnetic field prediction and making novel changes to reduce the computational burden of the exponential functions which a higher number of harmonics can be included in calculation.

The paper's structure is as follows; the problem is formulated in section 2. The drawn results are compared with FEM, in section 3. Finally, in the last section, the conclusion is made.

2. PROBLEM FORMULATION

To find an analytical answer, a set of assumptions should be considered to simplify the problem. It is assumed that the magnetic vector potential has only the z component, i.e., magnetic vector potential $\mathbf{A}$=[0, 0, $Az(x, y)$], because the magnetic flux density vector $\mathbf{B}$ and magnetic field intensity vector $\mathbf{H}$ have only perpendicular and tangential components. End effects are neglected. The magnetization vector of magnets does not have *z* component. The permeability of iron cores is considered as infinite [10, 11, 13]. The sides of the slots are along the y-axis. Eddy current is ignored.

As illustrated in Fig. 1, the domain of the problem is divided into mover core, PM, air gap, Ns slots and stator core regions based on the flux direction, machine geometry, and magnetic/electrical properties of each region. Ns is the slot's number. Generally, the following steps are required to calculate MFD distribution.

- In order to achieve an analytical solution, Neumann and continuous boundary conditions are defined.
- According to the assumptions and Maxwell's equations, the governing PDEs are derived for each subarea.
- The magnetization function is written as a Fourier series expansion.
- Depending on the kind of PDEs of each subarea, a homogenous and particular solution is found to satisfy the boundary conditions.
- To validate the method, the consistency of the results obtained is shown in comparison with FEM.

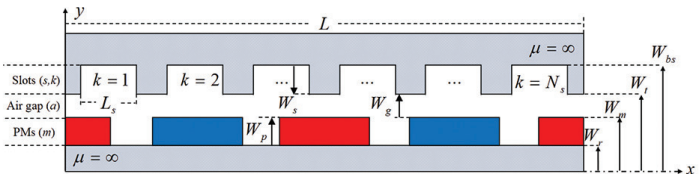

Fig. 1. Regions and spatial paprameters of the considered PMLSM

2.1. GOVERNING PARTIAL DIFFERENTIAL EQUATIONS

According to the basic principles of electromagnetism and Gauss's and Ampere's laws, as well as considering the defined sub-domains, Poisson's and Laplace's equations can be expressed as (1) and (2) in the open-circuit case.

$$\nabla^2 \mathbf{A}^i = 0,\ \mathrm{i}=\{a, s_k\}, k = 1,2,...,N_s \quad (1)$$

$$\nabla^2 \mathbf{A}^m = -\mu_0 \nabla \times \mathbf{M} \tag{2}$$

where $\mu 0$ is the free space magnetic permeability, and $\boldsymbol{M}$=[$Mx(x)$, $My(y)$, 0] is the magnetization vector. In (1) and (2), the air gap, slots and magnet regions are indicated by superscripts a, s_k, and m, respectively. (1) and (2) can be rewritten as

$$\frac{\partial^2 A_z^a}{\partial x^2} + \frac{\partial^2 A_z^a}{\partial y^2} = 0 \tag{3}$$

$$\frac{\partial^2 A_z^{s,k}}{\partial x^2} + \frac{\partial^2 A_z^{s,k}}{\partial y^2} = 0 \,,\; k = 1,2,...,N_s \tag{4}$$

$$\frac{\partial^2 A_z^m}{\partial x^2} + \frac{\partial^2 A_z^m}{\partial y^2} = \mu_0 \left(\frac{\partial M_x}{\partial y} - \frac{\partial M_y}{\partial x} \right) \tag{5}$$

2.2. BOUNDARY CONDITIONS

In this study, two types of boundary conditions are considered [10, 14]. 1) Neumann's boundary condition, 2) Continuous boundary condition which can be mathematically expressed as

$$\boldsymbol{n} \cdot \left(\boldsymbol{B}^{i-} - \boldsymbol{B}^{i+} \right) = 0 \tag{6}$$

$$\boldsymbol{n} \times \left(\boldsymbol{H}^{i-} - \boldsymbol{H}^{i+} \right) = 0 \tag{7}$$

$$\boldsymbol{n} \times \boldsymbol{H} = 0 \tag{8}$$

$\boldsymbol{n}$ is the normal unit vector at the interface between two adjacent regions, i.e., i+, i-. According to Neumann's boundary condition, the derivative of an unknown function has a certain value on a given boundary. Therefore, the perpendicular component of $\boldsymbol{H}$ vector at PM region at the boundary adjacent to mover back iron with infinite permeability and the tangential component of magnetic field intensity on both sides of slots adjacent to stator iron with infinite permeability should be zero. Also, the tangential component of $\boldsymbol{H}$ vector is zero at the slots's bottom.

$$H_x^m(x,y)\Big|_{y=W_r} = \frac{1}{\mu_0 \mu_r} \frac{\partial A_z^m(r,\theta)}{\partial y}\Big|_{y=W_r} = 0 \tag{9}$$

$$H_y^s(x,y)\Big|_{x=x_{ck} \pm \frac{a_s L}{2Ns}} = \frac{-1}{\mu_0} \frac{\partial A_z^s(x,y)}{\partial x}\Big|_{x=x_{ck} \pm \frac{a_s L}{2Ns}} = 0 \tag{10}$$

$$H_x^s(x,y)\Big|_{y=W_{bs}} = \frac{1}{\mu_0} \frac{\partial A_z^s(x,y)}{\partial y}\Big|_{y=W_{bs}} = 0 \tag{11}$$

The perpendicular component of $\boldsymbol{B}$ vector and the tangential component of $\boldsymbol{H}$ vector are continuous at the boundary between the PM region and the airgap, as well as at the boundary of the airgap and slot.

$$B_y^m(x,y)\Big|_{y=W_m} = B_y^a(x,y)\Big|_{y=W_m} \tag{12}$$

$$H_x^m(x,y)\Big|_{y=W_m} = H_x^a(x,y)\Big|_{y=W_m} \tag{13}$$

$$B_y^a(x,y)\Big|_{y=W_t} = B_y^s(x,y)\Big|_{y=W_t} \tag{14}$$

$$H_x^a(x,y)\Big|_{y=W_t} = \begin{cases} \sum_{k=1}^{\infty} H_x^s(x,y)\Big|_{x_c^k - L_s \le x \le x_c^k + L_s}^{y=W_t} \\ 0 \qquad \text{otherwise} \end{cases} \tag{15}$$

$$L_s = \frac{a_s L}{2N_s} \;,\; x_c^k = \frac{L}{2N_s}(1-a_s) + \frac{L_s}{2} + (k-1)L_s \;,\; k = 1,2,...,N_s$$

2.3. OPEN-CIRCUIT GENERAL SOLUTIONS

To find an analytical solution to Poisson's equations, the magnetization vector of the magnets must be available. In Cartesian coordinates, the magnetization vector can be defined as

$$\boldsymbol{M} = M_x(x)\hat{a}_x + M_y(x)\hat{a}_y \tag{16}$$

where $\hat{a}_x$ and a $\hat{a}_y$ are the unit vectors along the x and y axis. According to Fig. 2, since the parallel type of the magnetization pattern is considered, M_x and M_y can be expressed in terms of their Fourier series expansions as

$$\begin{aligned} M_y(x) &= \sum_{h=1}^{\infty} M_{yh} \cos\left(\tfrac{h\pi p}{L/2} (x - x_r) \right) \\ &= \sum_{h=1}^{\infty} \left[M_{yh} \cos\left(\tfrac{h\pi p}{L/2} x_r \right) \right] \times \cos\left(\tfrac{h\pi p}{L/2} x \right) \\ &+ \sum_{h=1}^{\infty} \left[M_{yh} \sin\left(\tfrac{h\pi p}{L/2} x_r \right) \right] \times \sin\left(\tfrac{h\pi p}{L/2} x \right) \end{aligned} \tag{17}$$

$$M_{yh} = \frac{2B_r}{\mu_0 h\pi} \left[\sin(h\pi/2) + \sin\left(h\pi(1 - \frac{a_p}{2}) \right) \right] \tag{18}$$

$$M_x(x) = 0 \tag{19}$$

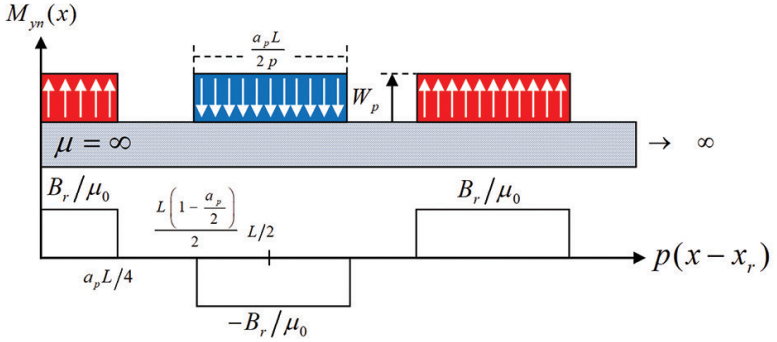

Fig. 2. Parallel magnetization Pattern. Note that $M_x(x)$=0.

where B_r is PM remanence flux density, a_p is the PM width per pole pitch ratio, M_{yh} is the hth element of $M_y(x)$, and $x_r=v_t+x_0$ is the spatial position of the mover where x_0 is its initial position.

In the case of open-circuit field prediction, if n=hp the homogeneous and particular solutions of the Poisson's equation in the permanent magnet area are expressed as

$$\mathbf{A}^m_{z,h}(x,y)= \sum_{n=1}^{\infty}\left\{\left[a_n^m e^{\frac{2n\pi}{L}y}+b_n^m e^{\frac{-2n\pi}{L}y}\right]\times\sin\left(\frac{2n\pi}{L}x\right) +\left[c_n^m e^{\frac{2n\pi}{L}y}+d_n^m e^{\frac{-2n\pi}{L}y}\right]\times\cos\left(\frac{2n\pi}{L}x\right)\right\} \tag{20}$$

$$\mathbf{A}^m_{z,p}(x,y)= \sum_{n=1}^{\infty}\left\{\begin{array}{l}\left[\mu_0\frac{L}{2h\pi}M_{yh}\sin\left(\frac{2h\pi}{L}x_r\right)\cos\left(\frac{2n\pi}{L}x\right)\right]+\\ \left[-\mu_0\frac{L}{2h\pi}M_{yh}\cos\left(\frac{2h\pi}{L}x_r\right)\right]\sin\left(\frac{2n\pi}{L}x\right)\end{array}\right\} \tag{21}$$

Applying the boundary condition (9) yields

$$\begin{aligned}\mathbf{A}^m_z(x,y)=&\sum_{n=1}^{N}\left\{\frac{-\mu_0 L}{2n\pi}M_{yh}\cos\left(\frac{2n\pi}{L}x_r\right)+\right.\\ &\left.a_n^m\left[e^{\frac{2n\pi}{L}y}+e^{\frac{4n\pi}{L}W_r}e^{\frac{-2n\pi}{L}y}\right]\right\}\times\sin\left(\frac{2n\pi}{L}x\right)\\ &+\sum_{n=1}^{N}\left\{\frac{\mu_0 L}{2n\pi}M_{yh}\sin\left(\frac{2n\pi}{L}x_r\right)+\right.\\ &\left.c_n^m\left[e^{\frac{2n\pi}{L}y}+e^{\frac{4n\pi}{L}W_r}e^{\frac{-2n\pi}{L}y}\right]\right\}\times\cos\left(\frac{2n\pi}{L}x\right)\end{aligned} \tag{22}$$

The solution of PDEs at the airgap and slots are expressed as

$$\sum_{n=1}^{N}\left\{\left[a_n^a e^{\frac{2n\pi}{L}y}+b_n^a e^{\frac{-2n\pi}{L}y}\right]\times\cos\left(\frac{2n\pi}{L}x\right) +\left[c_n^a e^{\frac{2n\pi}{L}y}+d_n^a e^{\frac{-2n\pi}{L}y}\right]\times\sin\left(\frac{2n\pi}{L}x\right)\right\} \tag{23}$$

$$\mathbf{A}^{s,k}_z(x,y)=\sum_{u=1}^{U}\left\{\left[a_u^{s,k}e^{\frac{u\pi}{L_s}y}+b_u^{s,k}e^{\frac{-u\pi}{L_s}y}\right] \times\cos\left(\frac{u\pi}{L_s}\left(x-x_c^k+\frac{L_s}{2}\right)\right)\right\} \tag{24}$$

For ease of the numerical computation, the equation (24) can be rewritten as

$$\mathbf{A}^{s,k}_z(x,y)= \sum_{u=1}^{U}\left\{\left[a_u^{s,k}e^{\frac{-u\pi}{L_s}W_{bs}}e^{\frac{u\pi}{L_s}y}+b_u^{s,k}e^{\frac{u\pi}{L_s}W_s}e^{\frac{-u\pi}{L_s}y}\right] \times\cos\left(\frac{u\pi}{L_s}\left(x-x_c^k+\frac{L_s}{2}\right)\right)\right\} \tag{25}$$

Applying the boundary condition (11) yields

$$\mathbf{A}^{s,k}_z(x,y)= \sum_{u=1}^{U}\left\{a_u^{s,k}\left[e^{\frac{-u\pi}{L_s}W_{bs}}e^{\frac{u\pi}{L_s}y}+e^{\frac{u\pi}{L_s}(W_{bs}-W_s)}e^{\frac{-u\pi}{L_s}y}\right] \times\cos\left(\frac{u\pi}{L_s}\left(x-x_c^k+\frac{L_s}{2}\right)\right)\right\} \tag{26}$$

2.4. APPLYING BOUNDARY CONDITIONS TO CALCULATE INTEGRATION CONSTANTSTEGRATION CONSTANTS

Based on the obtained equations, the number of integration constants is $6N+N_sU$, where N and U are the number of harmonics used in the general solutions for magnet, air gap and slot areas, respectively. In order to calculate integration constants, the boundary conditions stated in (12-15) must be applied.

Using the boundary condition (12), yields

$$\begin{aligned}&\frac{2n\pi}{L}a_n^m\left[e^{\frac{2n\pi}{L}W_m}+e^{\frac{2n\pi}{L}(2W_r-W_m)}\right]\\ &-\frac{2n\pi}{L}\left[c_n^a e^{\frac{2n\pi}{L}W_m}+d_n^a e^{\frac{-2n\pi}{L}W_m}\right]=\mu_0 M_{yn}\cos\left(\frac{2n\pi}{L}x_r\right)\end{aligned} \tag{27}$$

$$\begin{aligned}&\frac{2n\pi}{L}c_n^m\left[e^{\frac{2n\pi}{L}W_m}+e^{\frac{2n\pi}{L}(2W_r-W_m)}\right]\\ &-\frac{2n\pi}{L}\left[a_n^a e^{\frac{2n\pi}{L}W_m}+b_n^a e^{\frac{-2n\pi}{L}W_m}\right]=-\mu_0 M_{yn}\sin\left(\frac{2n\pi}{L}x_r\right)\end{aligned} \tag{28}$$

Applying the boundary condition (13) yields

$$\begin{aligned}&c_n^m\left[e^{\frac{2np\pi}{L}W_m}-e^{\frac{2np\pi}{L}(2W_r-W_m)}\right]\\ &-\left[a_n^a e^{\frac{2n\pi}{L}W_m}-b_n^a e^{\frac{-2n\pi}{L}W_m}\right]=0\end{aligned} \tag{29}$$

$$\begin{aligned}&a_n^m\left[e^{\frac{2np\pi}{L}W_m}-e^{\frac{2np\pi}{L}(2W_r-W_m)}\right]\\ &-\left[c_n^a e^{\frac{2n\pi}{L}W_m}-d_n^a e^{\frac{-2n\pi}{L}W_m}\right]=0\end{aligned} \tag{30}$$

$$\begin{aligned}&\left(-\frac{u\pi}{L_s}\right)\left\{a_u^{s,k}\left[e^{\frac{u\pi}{L_s}W_t}+1\right]\right\}\\ &+\sum_{n=1}^{N}\frac{2n\pi}{L}\left\{\left[a_n^a e^{\frac{2n\pi}{L}W_t}+b_n^a e^{\frac{-2n\pi}{L}W_t}\right]\right.\\ &\times\frac{2}{L_s}\int_{x_c^k-\frac{L_s}{2}}^{x_c^k+\frac{L_s}{2}}\sin\left[\frac{u\pi}{L_s}\left(x-x_c^k+\frac{L_s}{2}\right)\right]\sin\left(\frac{2n\pi}{L}x\right)dx\\ &\left.-\left[c_n^a e^{\frac{2n\pi}{L}W_t}+d_n^a e^{\frac{-2n\pi}{L}W_t}\right]\right.\\ &\left.\times\frac{2}{L_s}\int_{x_c^k-\frac{L_s}{2}}^{x_c^k+\frac{L_s}{2}}\sin\left[\frac{u\pi}{L_s}\left(x-x_c^k+\frac{L_s}{2}\right)\right]\cos\left(\frac{2n\pi}{L}x\right)dx\right\}\end{aligned} \tag{31}$$

Applying the boundary condition (15) and using the correlation technique, yields

$$\frac{2n\pi}{L}\left[-a_n^a e^{\frac{2n\pi}{L}W_t}+b_n^a e^{\frac{-2n\pi}{L}W_t}\right]+\sum_{k=1}^{N_s}\sum_{u=1}^{U}\frac{u\pi}{L_s}\left\{a_u^{s,k}\left[e^{\frac{u\pi}{L_s}W_t}-1\right]\times\frac{2}{L_s}\int_{x_c^k-\frac{L_s}{2}}^{x_c^k+\frac{L_s}{2}}\cos\left[\frac{u\pi}{L_s}\left(x-x_c^k+\frac{L_s}{2}\right)\right]\cos\left(\frac{2n\pi}{L}x\right)dx\right\}=0 \quad (32)$$

$$\frac{2n\pi}{L}\left[-c_n^a e^{\frac{2n\pi}{L}W_t}+d_n^a e^{\frac{-2n\pi}{L}W_t}\right]+\sum_{k=1}^{N_s}\sum_{u=1}^{U}\frac{u\pi}{L_s}\left\{a_u^{s,k}\left[e^{\frac{u\pi}{L_s}W_t}-1\right]\times\frac{2}{L_s}\int_{x_c^k-\frac{L_s}{2}}^{x_c^k+\frac{L_s}{2}}\cos\left[\frac{u\pi}{L_s}\left(x-x_c^k+\frac{L_s}{2}\right)\right]\sin\left(\frac{2n\pi}{L}x\right)dx\right\}=0 \quad (33)$$

Finally, since $\boldsymbol{B}=\nabla\times\boldsymbol{A}$, the air-gap MFD can be expressed as

$$B_y^a(x,y)=\sum_{n=1}^{N}\left\{\frac{2n\pi}{L}\left[a_n^a e^{\frac{2n\pi}{L}W_{gm}}+b_n^a e^{\frac{-2n\pi}{L}W_{gm}}\right]\times\sin\left(\frac{2n\pi}{L}x\right)+\frac{2n\pi}{L}\left[c_n^a e^{\frac{2n\pi}{L}W_{gm}}+d_n^a e^{\frac{-2n\pi}{L}W_{gm}}\right]\times\cos\left(\frac{2n\pi}{L}x\right)\right\} \quad (34)$$

$$B_x^a(x,y)=\sum_{n=1}^{N}\left\{\frac{2n\pi}{L}\left[a_n^a e^{\frac{2n\pi}{L}W_{gm}}-b_n^a e^{\frac{-2n\pi}{L}W_{gm}}\right]\times\cos\left(\frac{2n\pi}{L}x\right)+\frac{2n\pi}{L}\left[c_n^a e^{\frac{2n\pi}{L}W_{gm}}-d_n^a e^{\frac{-2n\pi}{L}W_{gm}}\right]\times\sin\left(\frac{2n\pi}{L}x\right)\right\} \quad (35)$$

where W_{gm} is the air-gap middle width.

3. CASE STUDIES

Two slotted PMLSMs with parallel magnets have been considered to clarify the functionality of the presented approach. The results obtained from FEM and analytical method are compared.

FEM is a powerful numerical method for the analysis of electrical machines, in which the problem domain is discretized into finite elements by meshing and the governing equation for each element is solved numerically. Therefore, the quality of the mesh is critical in FEA and directly affects the accuracy of the results. To increase the accuracy, a denser mesh pattern should be used for the air gap region. ANSYS MAXWELL was used to model and analyze the considered PMLSMs.

The parameters of the considered PMLSMs are given in Table 1. The perpendicular and tangential components of the open-circuit magnetic flux density at the air-gap centerline are illustrated in Figs. 3–6. As it is obvious, the results obtained from the proposed method are very similar to that of obtained by the FEM. Figs. 3 and 4 illustrate the obtained results, respectively, for two different mover positions of the first studied motor, i.e. x_0=0 and x_0=L/3. Similar results for the second studied motor are shown in Figs. 5 and 6 at different mover positions, i.e. x_0=0 and x_0=L/5.

Table 1. Parameters of the considered PMLSMs

Parameter	Explanation	Value (1st motor)	Value (2nd motor)	Unit
W_r	Mover core thickness	0.012	0.012	(m)
W_p	PM height	0.005	0.005	(m)
W_g	Air-gap length	0.001	0.001	(m)
W_s	Slots height	0.025	0.025	(m)
L	Motor length	0.216	0.2	(m)
B_r	PM remanence flux density	1.23	1.23	(T)
N_s	Number of stator slots	9	12	-
p	Number of pole pairs	4	2	-
a_s	Slot width to slot pitch ratio	0.54	0.6	-
a_p	PM width to pole pitch ratio	0.7	0.8	-

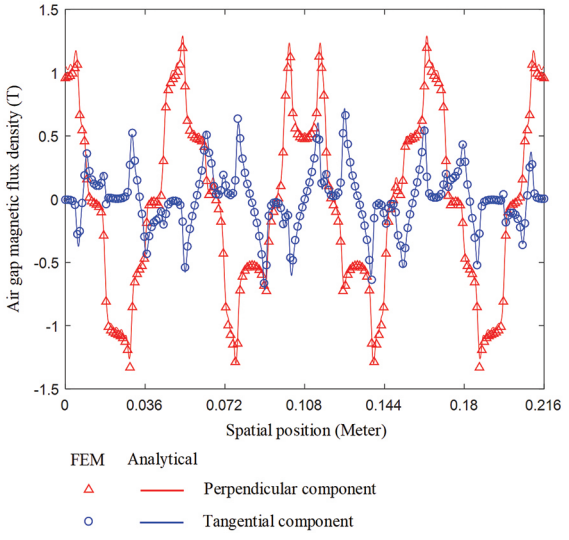

Fig. 3. Components of air-gap MFD obtained for the first linear motor (x_0=0)

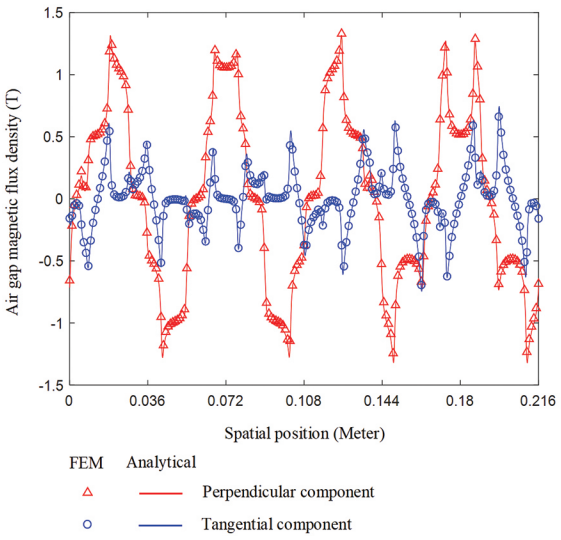

Fig. 4. Components of air-gap MFD obtained for the first linear motor (x_0=L/3)

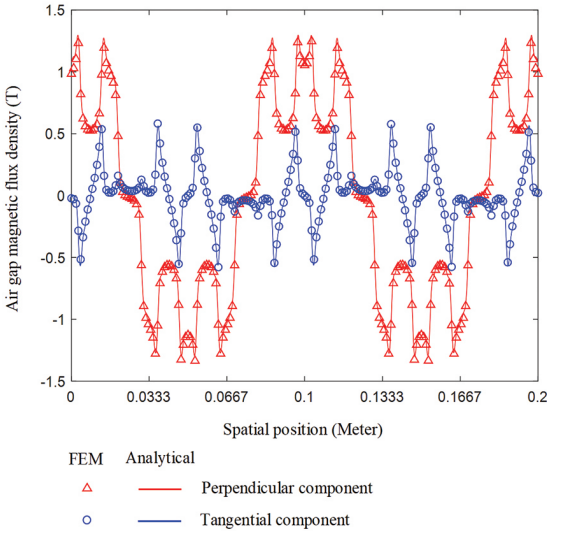

Fig. 5. Components of air-gap MFD obtained for the second linear motor (x_0=0)

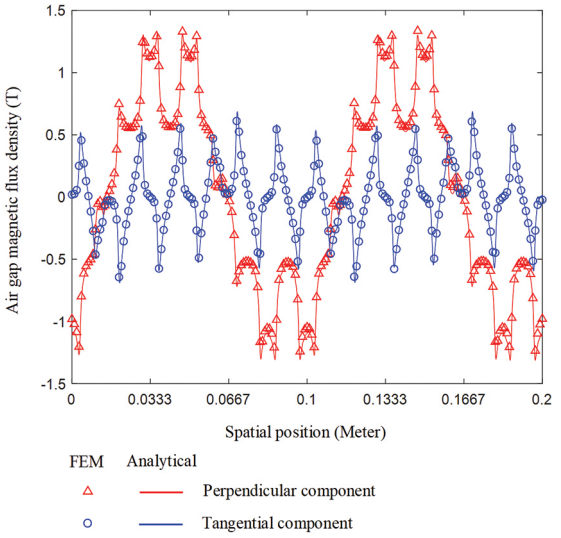

Fig. 6. Components of air-gap MFD obtained for the second linear motor (x_0=L/5)

4. CONCLUSIONS

Analytical methods based on mathematical equations can be an effective tool in optimization processes due to the reduction of the computational volume, provided that the simplifications made do not sacrifice the accuracy of the problem. In this paper, open-circuit magnetic field is calculated analytically for slotted PMLSMs with surface-mounted magnets. The parallel magnetization pattern is used and the Poisson's/Laplace's equations are expressed for all regions to calculate the magnetic field distribution. Two different PMLSMs with (8-pole, 9-slot) and (4-pole, 12-slot) are considered as case studies and the results are verified by FEM. These solutions can also be used to calculate the crucial quantities of the machine such as back-EMF and cogging force. For further studies, it is recommended that this method be extended to armature reaction field calculations.

5. REFERENCES:

[1] Y. Zhou, R. Qu, D. Li, Y. Gao, C. H. T. Lee, "Performance investigation and improvement of linear vernier permanent magnet motor for servo application", IEEE/ASME Transactions on Mechatronics, Vol. 28, No. 5, 2023, pp. 2657-2669.

[2] K. H. Kim, D. K. Woo, "Linear tubular permanent magnet motor for an electromagnetic active suspension system", IET Electric Power Applications, Vol. 19, No. 12, 2021, pp. 1648-1665.

[3] Y. Shen, Z. Zeng, Q. Lu, C. H. T. Lee, "Design and analysis of double-sided flux concentrated permanent magnet linear machine with saturation relieving effect", IEEE Transactions on Industrial Electronics, Vol. 70, No. 10, 2023, pp. 10442-10453.

[4] F. Cui, Z. Sun, W. Xu, W. Zhou, Y. Liu, "Comparative analysis of bilateral permanent magnet linear synchronous motors with different structures", CES Transactions on Electrical Machines and Systems, Vol. 4, No. 2, 2020, pp. 142-150.

[5] X. Liu, J. Gao, S. Huang, K. Lu, "Magnetic field and thrust analysis of the U-channel air-core permanent magnet linear synchronous motor", IEEE Transactions on Magnetics, Vol. 53, No. 6, 2017.

[6] D. Pan, L. Li, M. Wang, "Modeling and optimization of air-core monopole linear motor based on multiphysical fields", IEEE Transactions on Industrial Electronics, Vol. 65, No. 12, 2018, pp. 9814-9824.

[7] Z. Li et al. "Hybrid analytical model of permanent magnet linear motor considering iron saturation and end effect", IEEE Transactions on Energy Conversion, Vol. 39, No. 3, 2024, pp. 2008-2017.

[8] B. Li, J. Zhang, X. Zhao, Z. Miao, Z., H., H. Li, "Magnetic Field Analysis of Trapezoidal Halbach Permanent Magnet Linear Synchronous Motor Based on Improved Equivalent Surface Current Method", Applied Computational Electromagnetics Society Journal, Vol. 40, No. 1, 2025, pp. 69-78.

[9] E. Kazan,A. Onat, "Modeling of air core permanent-magnet linear motors with a simplified nonlinear magnetic analysis", IEEE Transactions on Magnetics, Vol. 47, No. 6, 2011, pp. 1753-1762.

[10] A. Rahideh, A. Ghaffari, A. Barzegar,A. Mahmoudi, "Analytical model of slotless brushless pm linear motors considering different magnetization patterns", IEEE Transactions on Energy Conversion, Vol. 33, No. 4, 2018, pp. 1797-1804.

[11] H. Hu, J. Zhao, X. Liu, Y. Guo, "Magnetic field and force calculation in linear permanent-magnet synchronous machines accounting for longitudinal end effect", IEEE Transactions on Industrial Electronics, Vol. 63, No. 12, 2016, pp. 7632-7643.

[12] S. G. Min, B. Sarlioglu, "3-D performance analysis and multiobjective optimization of coreless-type PM linear synchronous motors", IEEE Transactions on Industrial Electronics, Vol. 65, No. 2, 2017, pp. 1855-1864.

[13] K. Atallah, Z. Q. Zhu, D. Howe, "Armature reaction field and winding inductances of slotless permanent-magnet brushless machines", IEEE Transactions on Magnetics, Vol. 34, No. 5, 1998, pp. 3737-3744.

[14] B. Gysen, K. Meessen, J. Paulides, E. Lomonova, "General formulation of the electromagnetic field distribution in machines and devices using Fourier analysis", IEEE Transactions on Magnetics, Vol. 46, No. 1, 2009, pp. 39-52.